UNIABUJA Journal of Engineering and Technology

https://ujet.uniabuja.edu.ng/

ISSN: 2714-3236 (Online); 2714-3228 (Print)

Volume 3, Issue 1, 2026; 250-258

Simulation of an Improved Road-Side Maize Roasting Machine and Thermal Efficiency Validation

Michael M. ODEWOLE[1*], Sodiq A. OLALEYE[2], Muhminah T. ABDULRAHMAN[3], Onyinyechi E.-G. ONYEMACHI[4], Faith O. ADEOTI[5]

[1,3,4]*Department of Food Engineering, Faculty of Engineering and Technology, University of Ilorin, Ilorin, Nigeria*
[2,5]*Department of Agricultural and Biosystems Engineering, Faculty of Engineering and Technology, University of Ilorin, Ilorin, Nigeria*

[1*]*odewole.mm@unilorin.edu.ng*, [2]*olasodiq@gmail.com*, [3]*temidunabdulrahman@gmail.com*, [4]*akhereonyinyechi@gmail.com*, [5]*faith.adeoti2002@gmal.com*

Abstract

The study focused on the simulation of temperature distribution, air flow pattern, and validation of the thermal efficiency of an improved road-side maize roasting machine. SolidWorks Premium SP1.2 2025 Computational Fluid Dynamics (CFD) software was used for modelling and simulation operations. The thermal efficiency validation was done by estimating the efficiency of the fabricated prototype of the machine (through a standard experiment of roasting), and comparing with that of simulated model of the machine. The simulation results showed that, the modelled machine performed best in terms of temperature distribution and air flow of the roasting region at the point 1.7 m cut plot (other points: 1.5 m and 1.6 m), with average temperature and average air velocity of 498.30±2.34 °C and 1.079±0.19 m/s, respectively. However, the overall average temperature and overall average air velocity obtained were 463.13±56.11 °C and 0.962±0.17 m/s, respectively. Also, the thermal efficiency of the simulated model of the machine was 93% and that of fabricated prototype of the machine was 66%. This revealed that, the fabricated machine requires future modifications to enhance better thermal efficiency of the roasting operation.

Keywords: *Maize roasting, simulation, computational fluid dynamics, forced convection, efficiency.*

1.0 Introduction

Maize (*Zea mays*) is an important crop used for food and fodder in many countries. It is the third globally produced grain after rice and wheat (Lisa *et al*., 2019). As an annual crop, it belongs to the family *Poaceae* (Saeed and Saeed, 2020), which is a good source of energy and phytochemicals, such as phenolic compounds, carotenoids and phytosterols (Saeed and Saeed, 2020).

Roasting is a cooking method that involves drying out foods, such as grains or nuts, by exposing them to direct heat, typically in an oven or over an open fire (Jimoh *et al*., 2020). This process removes excess moisture, softens and prepares the food for safe consumption (Jimoh *et al*., 2020). It is also used as a heat treatment to inactivate pathogens and microorganisms, extend shelf life, ensure food safety, and to ensure desired sensory properties such as texture, colour, aroma and flavour (Szpicer *et al*., 2025). However, factors such as the type of food material and the processing conditions, which include time and temperature, greatly affect the food's nutritional content (Sruthi *et al*., 2021). Furthermore, the effect of roasting includes increased antioxidant activity, development of brown colouration and improved flavour due to the presence of Maillard reaction in products. These changes contribute to better health benefits by enhancing the digestibility of nutrients and activity of available antioxidants (Oladeji, 2022).

Maize roasting involves placing maize cobs on a grill, above hot charcoal and regularly turning it for even cooking (Atere *et al*., 2020). Traditionally, maize is roasted along with its husk by directly placing into a fire and its removal after the cob might have been slightly burnt (Adeyinka *et al*., 2014). Roadside roasting of maize in Nigeria with the use of charcoal and metallic grill is an age long practice. However, this method is prone to massive heat loss, leading to low thermal efficiency, drudgery, low productivity, and somewhat unhygienic due to direct touching of maize with bare hands and exposure to smoke and ash from the burning charcoal. Ogunlade and Sangosina (2019) reported the design, fabrication and testing of a maize roaster. The average time for effective roasting was in the range of 120-150 seconds. Kigozi *et al*. (2020) caried out a study on the design and thermal performance of soybean roaster with charcoal as the energy source. It was observed that the lower the distance between the drum (roasting chamber) and the stove (heat source), the greater the temperature of the drum.

Simulation is the science of creating a model to imitate an existing system, testing the models to observe its behavior, so as to understand, generalize and make a conclusion on the factors that influence the

Received: 17-01-2026 / Accepted: 02-02-2026 / Published: 31-03-2026

https://doi.org/10.70118/ujet.2026.0301.23

performance of the model (Lamé and Simmons, 2018; White and Ingalls, 2015). Simulation is used to improve performances of a system, justifying the use of resources, cost and time (Silva *et al*., 2010). There are two types of simulation model, which is the continuous simulation and discrete event simulation. Continuous simulation model is used for systems that has variables that changes continuously with time, the results of this simulation is taken at fixed time intervals. Discrete event simulation is used for systems in which its variables change at specific points in time (Bandyopadhyay and Bhattacharya, 2014; Özgün and Barlas, 2009). Simulation is applied for use in objects and procedures, for example, an ellipsoid object was used to create a model in order to simulate a coffee bean roaster, also physicians use simulated patients to learn new procedures(Chiang *et al*., 2017; White and Ingalls, 2015). The methods of simulation involves creating a conceptual design, using a software, validating the design to know how close it is to the original design, designing of experiments, implementing the design, analyzing the results, and then interpreting the results (Dooley, 2017).

The use of computational fluid dynamics (CFD) as a tool for simulation has become indispensable in the food industry. It provides detailed insights into the intricate transport phenomena, which takes place during food processing by modelling the flow of fluid, heat and mass transfer with high precision. This enables optimisation of processes, prediction of temperature distribution and patterns of flow, which are crucial in ensuring the quality and safety of products (Szpicer *et al*., 2025). Szpicer *et al*. (2023) reported that computational fluid dynamics (CFD) had been used to demonstrate the simulation of the drying of by-products of distillation operation, and its viability in other industrial applications and how CFD can accurately simulate complex drying processes and improve the advancement of food processing technology. Szpicer *et al*. (2023) further reported the use of computational fluid dynamics model for microwave-assisted fluidized bed drying of soybean. The model was able to evaluate and accurately predict the drying process. Fachruddin *et al*. (2021) simulated coffee roasting machine. It was established that simulated temperatures were lower than the validated values. However, consistent simulated patterns were displayed in temperature distribution.

Researchers have designed and simulated various food roasters (Atere, *et al*., 2020; Ogunlade and Sangosina, 2019; Chiang *et al*., 2017; Dash *et al*., 2019; Fachruddin *et al*., 2021; Kigozi *et al*., 2020), however, there is scarcity of information on the simulation of a road-side maize roasting machine. Therefore, the objective of this study was to use CFD approach to simulate the temperature distribution and air flow pattern of an improved road-side maize roasting machine. The outcomes will lead to having a better understanding of the major roasting parameters of the machine before its real-life fabrication for intended use.

2.0 Materials and Methods

2.1 Description of the machine

Figures 1(a) and 1(b) show the orthographic, and exploded views of the improved road-side maize roasting machine. The major components of the machine are: structural frame made of mild steel (40 mm by 40mm), structural frame coverings made of stainless steel 304, pulleys (250 mm and 50mm), pillow bearings, blower, solid shaft (20 mm), ash tray (260 mm by 285 mm), heat resistant rope (1295.04 mm), roasting frame (352 mm by 374 mm), charcoal tray (255 mm by 280 mm), roasting mesh (260 mm by 280 mm) and holding mesh (260 mm by 380 mm). The charcoal powered maize roasting machine was modelled in SolidWorks Premium SP1.2 2025. Individual components were created in the part environment, and then assembled in the Assembly environment of the CAD software.

The roasting mesh is situated 155 mm from the top of the roasting machine. Heat is generated in a charcoal tray located 100 mm beneath the roasting tray. The charcoal tray was designed to hold the charcoal efficiently, ensuring optimal combustion and heat transfer. An ash tray is positioned 177 mm directly beneath the charcoal compartment to collect ash conveniently, and facilitate easy clean-up after operation. A holding mesh, held by two rods of 400 mm length was designed to hold the maize after roasting. The insulating material chosen to prevent heat loss was fibre glass. The manually operated centrifugal blower was for moving heated air from the hot charcoal to the maize roasting mesh effectively. It is linked to two pulleys with a heat-resistant rope to achieve 1:5 speed ratio. The big (driving) pulley is fixed to the structural frame with the solid shaft and pillow bearing, while the small (driven) pulley is on the blower.

2.2 Working principle of the machine

The machine basically operates on the principle of convective heat transfer, under forced condition. The mass, momentum, and energy conserved in fluid (heated air), as explained with Navier-Stoke equation governed the working of the machine (Szpicer *et al*., 2025). The heat generated by the combusting charcoal is forcefully moved vertically (via manual rotation of the big pulley linked to the blower with the rope) to the roasting mesh region, where the fresh maize cobs were arranged for roasting. This process also ensures faster rate of combustion of the charcoal, and high rate of heat transfer as air from the blower moves through the

Received: 17-01-2026 / Accepted: 02-02-2026 / Published: 31-03-2026

https://doi.org/10.70118/ujet.2026.0301.23

burning charcoal. The speed ratio (1:5) of the two (2) pulleys ensures less stress and reduces drudgery associated with the conventional method of road-side maize roasting operation. This means, one (1) complete revolution of the big pulley will make the small pulley on the blower to turn five (5) complete revolutions which gives the operator some time to rest and conserve energy, thereby reducing drudgery.

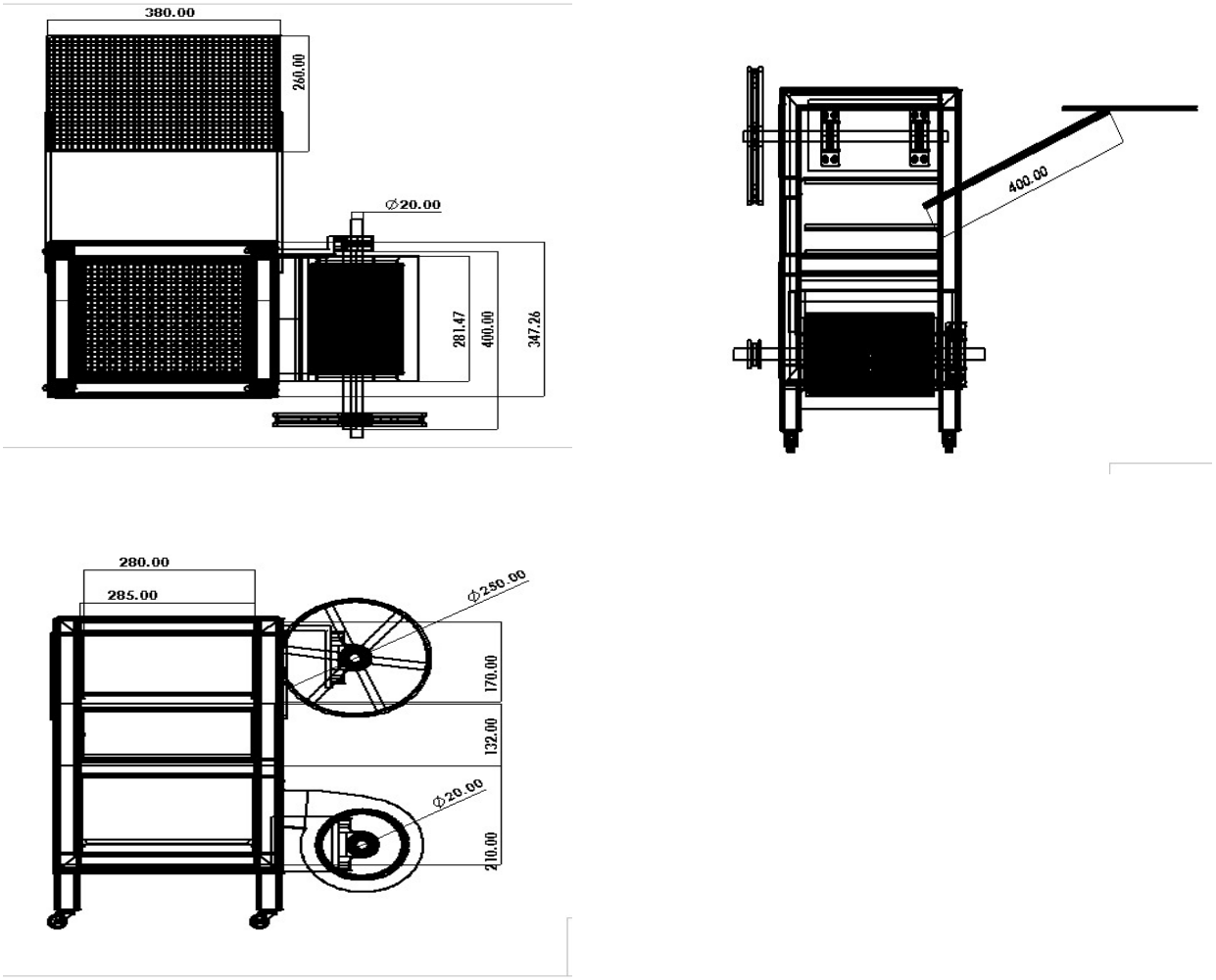

Figure 1(a): Orthographic view of the improved road-side maize roasting machine

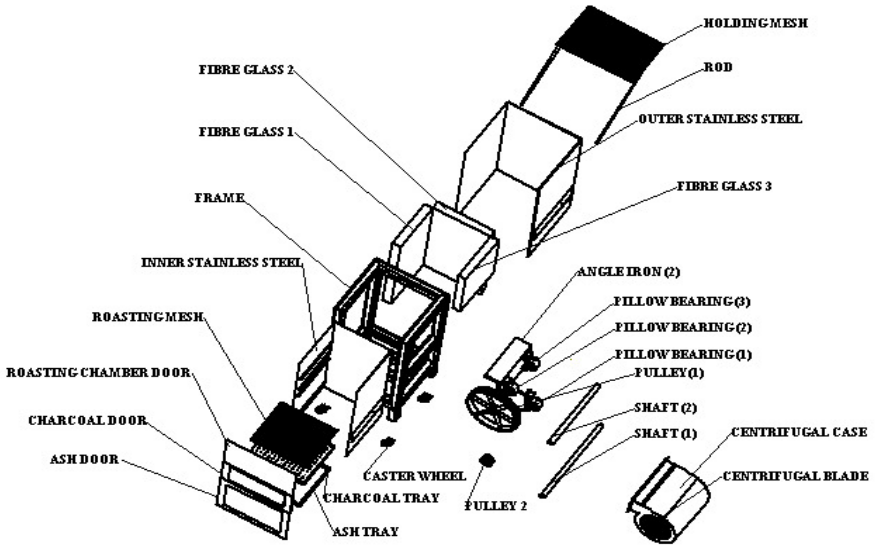

ITEM NO.	PART NUMBER	QTY.
1	FIBRE GLASS 1	1
2	Frame	1
3	FIBRE GLASS 2	1
4	FIBRE GLASS 3	1
5	Inner stainless sheet	1
6	Outer stainless steel	1
7	Ash tray	1
8	Charcoal tray	1
9	Roasting mesh	1
10	Roasting chamber door	1
11	Ash door	1
12	Angle iron (2)	1
13	Pillow bearing	3
14	Shaft (2)	1
15	Pulley (1)	1
16	Charcoal door	1
17	Centrifugal blade	1
18	Centrifugal case	1
19	Shaft (1)	1
20	Pulley 2	1
21	Angle iron	1
22	Holding mesh	1
23	Caster wheel (1)	4
24	Rod	2

Figure 1(b): Exploded view of the improved road-side maize roasting machine

Received: 17-01-2026 / Accepted: 02-02-2026 / Published: 31-03-2026

https://doi.org/10.70118/ujet.2026.0301.23

2.3 Model development

The machine (Figure 2) was modelled as a solid body, based on the assumption that the structural frame, the inner and outer stainless steels coverings are a single body. The multi-layer housing assembly comprising inner and outer stainless steel, fiberglass, and frame was modeled as a single geometric body to define the fluid domain boundary. This is because the simulation focuses strictly on fluid-side thermodynamics; consequently, the internal wall composition is decoupled from the flow solution, which is only required within the inner stainless-steel layer. The level of initial mesh was set at 5. The fluid domain of the modelled machine is as presented in Figure 3.

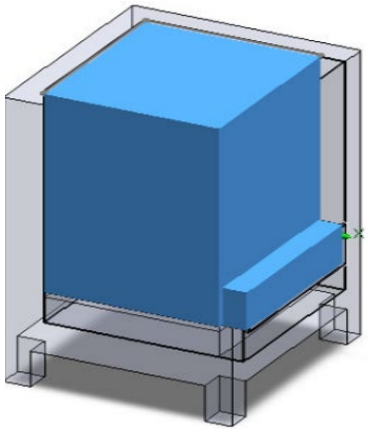

Figure 2: Developed model of the machine

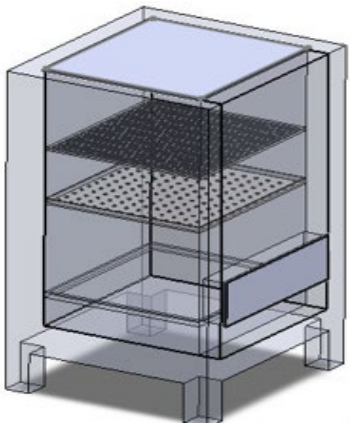

Figure 3: Fluid domain

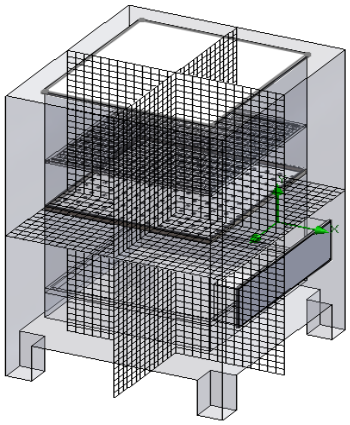

Figure 4: Discretisation of the machine

2.4 Simulation process

The modelled machine was subjected to simulation with the use of 2% standard turbulence intensity and 0.003 m of turbulence length. A value of 2% is a common, conservative assumption for internal duct flow which was applied here as a baseline in the absence of experimental fan data. The inlet turbulence length scale was defined as 0.003 m (3 mm) to represent the characteristic length scale of the turbulent structures shed from the trailing edge of the centrifugal fan blades and the volute tongue (cutoff) interaction. The simulation was done to study the temperature distribution and air flow patterns within the roasting machine. The three governing equations (Equations 1 – 3) that described Navier-Stokes equations (Odewole *et al*., 2017) were solved iteratively (159 iterations) using the SolidWorks Premium Flow Simulation 2025 SP1.2 based on the Finite Volume Method (FVM). To achieve accurate simulated results, the total cell count (27841), fluid cell (27841), Solid cells (14651), and partial cells (9211) were derived from the discretization process and subsequently used for analysis. The difference between the model and the experimental data was used to judge the reliability of the models used for analyzing the phenomena occurring inside the roasting machine. The initial conditions for the simulation are as presented in Table 1.

Continuity Equation:

$$\frac{\partial \rho}{\partial t} + \rho \frac{\partial U_i}{\partial x_i} = 0 \quad (1)$$

Where ρ is the fluid density, t is the time, U is the fluid velocity vector component, and x is the spatial coordinate

Received: 17-01-2026 / Accepted: 02-02-2026 / Published: 31-03-2026

https://doi.org/10.70118/ujet.2026.0301.23

Momentum Equation:

$$\rho \frac{\partial U_i}{\partial t} + \rho U_i \frac{\partial U_j}{\partial x_i} = -\frac{\partial P}{\partial x_j} - \frac{\partial \tau_{ij}}{\partial x_i} + \frac{\rho g_j}{V} \quad (2)$$

Where ρ is the fluid density, t is the time, U is the fluid velocity vector component, x is the spatial coordinate, P is the pressure, τ is the viscous stress tensor component, V is the volume, and g is the gravitational acceleration component

Energy Equation:

$$\rho c_\mu \frac{\partial T}{\partial t} + \rho c_\mu U_i \frac{\partial T}{\partial x_i} = -P \frac{\partial U_i}{\partial x_i} + \lambda \frac{\partial^2 T}{\partial x_i^2} - \tau_{ij} \frac{\partial U_i}{\partial x_i} \quad (3)$$

Where ρ is the fluid density, t is the time, U is the fluid velocity vector component, x is the spatial coordinate, P is the pressure, τ is the viscous stress tensor component, λ is the thermal conductivity, c_μ is the specific heat, and T is the temperature

Table 1: Initial and boundary conditions used for simulation

S/N	Parameter	Value
1	Initial temperature of charcoal bed	500 °C
2	Turbulence parameters	Intensity (2 %) and Length (0.003 m)
3	Thermodynamic parameters	Pressure (101325 Pa) and Temperature (30 °C)
4	Initial air temperature	30 ^{0}C
5	Fluid	Air
6	Direction of flow	Y axis
7	Inlet air velocity	0.95 m/s
8	Level of refinement of mesh	5
9	Initial velocity	0 m/s

2.5 Validation of simulated model: thermal efficiency

The performance of the simulated model (roasting machine) was done after the fabrication of a prototype version of the machine. The performance evaluation was carried out on the fabricated roasting machine to evaluate its thermal efficiency. An Infrared thermometer (non-contact; -50 to 650 °C; Field of view – Distance to target 12:1) was used to take the temperature readings. Fresh maize was roasted at an average temperature of 143 °C for 9 mins, and the temperature readings were taken at the inner and outer surfaces of the roasting machine and in all compartments (roasting, charcoal, and ash compartments). These temperature readings were used to estimate the heat generated, and heat lost. Thermal efficiency was then determined based on the empirical formula (Equation 4), useful heat absorbed, and total heat generated.

Thermal efficiency was calculated using equation 4 (Bora and Nakkeeran, 2014)

$$\eta = \frac{Q_{output}}{Q_{input}} \times 100\% \quad (4)$$

Where Q_{input} is the inside temperature of the charcoal compartment, and Q_{output} is the inside temperature of the roasting compartment.

3.0 Results and Discussion

3.1 Trajectories of air flow for temperature and velocity

Figures 4 (a and b) illustrate the flow trajectories of air temperature and the flow trajectories of air velocity inside the roasting chamber, respectively. These provide information about the behavior of the air from inlet to outlet. Flow paths (with 1000 data points) were examined to identify some of the significant features of flow. The movement of hot air upwards concentrates thermal energy in the space just above the bed. This optimal flow creates a high-temperature zone in-between the charcoal bed and the roasting mesh. Maximum air temperatures (30.04 - 500.07 ^{o}C) were observed to be located in-between the charcoal bed and the roasting mesh. Maximum air velocities (0.190 - 1.487 m/s) were observed to be around the inlet region, in-between the charcoal bed and roasting mesh, and at the sides close to the top of the solid model. The high air velocity at the inlet could be related to the location of the blower, which contributed to the high air flux. The high temperature between the charcoal bed and the roasting chamber region gave rise to expansion of the air (higher kinetic energy), hence the air velocity increased. The air velocity shows that the material directly placed on the roasting mesh receives the most intense and direct heat transfer due to surface contact. Odewole

Received: 17-01-2026 / Accepted: 02-02-2026 / Published: 31-03-2026

https://doi.org/10.70118/ujet.2026.0301.23

et al. (2017), in the simulation of hot air flow pattern in cabinet dryer, observed that temperature is highest at the center of the dryer and velocity is maximum at the inlet region.

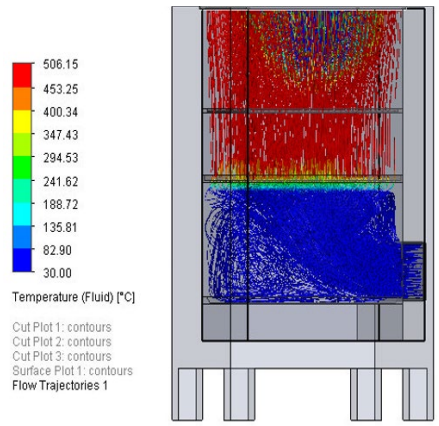

Figure 4(a): Flow Trajectories of Air Temperature

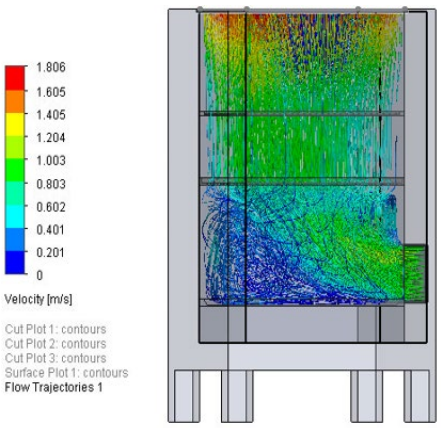

Figure 4 (b): Flow Trajectories of Air Velocity

3.2 Computational fluid dynamics for air temperature

In simulation of the roasting machine, dry air temperature inside the roasting chamber was estimated from front plane cut plot of temperature profile by three cut plots; cut plots (a, b and c) at three offsets (1.5, 1.6 and 1.7 m) respectively. Figure 5 represents the temperature cut plots at 1.5 m (a), 1.6 m (b) and 1.7 m (c) offsets. These figures illustrate that within the roasting machine, the area near the rear middle (cut plot at 1.6 m) had the lowest roasting temperature (about 30 °C), which contrasted sharply with the adjacent rear end sections (1.5 m and 1.7 m) that recorded significantly higher temperatures (466 °C to about 500 °C). This signifies a transfer of heat from the charcoal bed to the walls of the roasting chamber through conduction and the reduced atmospheric air access to the walls. This results to the air at the walls being significantly hotter than that at the center of the bed because of the convective heat transfer occurring between the walls and the air near it. Additionally, as the charcoal heat the air, it becomes less dense and rises along the walls, since temperature and density have an inverse correlation. Suryadi *et al*. (2024) analysed temperature distributions along a roaster drum using computational fluid dynamics (CFD) and reported that the highest temperature values are at edges of the drum. According to this simulation, the middle of the roasting chamber from above goes through a significant decrease in the hot air temperature. This could be attributed to the ambient inflow air charged to the chamber from its centre top. The maximum temperature achieved for the simulation is 506.15 °C while the minimum is 30 °C. The temperature of air at inlet is 30 - 40 °C. The average temperature obtained from the simulation was considerably higher than the experimental roasting average temperature (143 °C). However, the experimental value depicts the average temperature that gave the most preferred roasting. Table 2 shows the temperature in the roasting mesh's compartment is approximately 466 °C on an average.

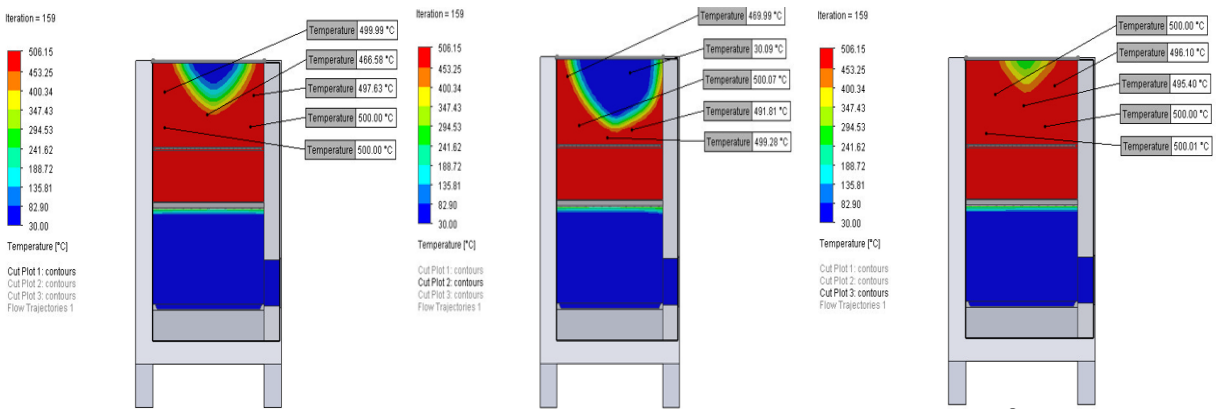

(a) (b) (c)

Figure 5: Temperature Cut Plots at 1.5 m (a), 1.6 m (b) and 1.7 m (c) offsets

Received: 17-01-2026 / Accepted: 02-02-2026 / Published: 31-03-2026

https://doi.org/10.70118/ujet.2026.0301.23

Table 2: Temperature in the roasting chamber at different points

S/N	Temperature (°C) at 1.5 m	Temperature (°C) at 1.6 m	Temperature (°C) at 1.7 m
1	499.99	469.99	500.00
2	466.58	30.04	496.10
3	497.63	500.07	495.40
4	500.00	491.81	500.00
5	500.00	499.28	500.01
	Average Temperature: 492.84±14.72	**Average Temperature: 398.24±206.19**	**Average Temperature: 498.30±2.34**
	Overall Avg. Temperature:	**463.13±56.11**	

3.3 Computational fluid dynamics for air velocity

Figure 6 indicates the air flow velocity cut plots at 1.5 m (a), 1.6 m (b), and 1.7 m (c) in the roasting machine. The velocity is high (0.190 - 1.487 m/s) as it enters the roasting machine and also as it approaches and enters the charcoal bed. The velocity was maximum 1.040±0.22 and 1.079±0.19 m/s at the offset of 1.5 and 1.7 m, respectively, and minimum at 1.6 m 0.767±0.49 m/s in the roasting chamber. The observed increase in air velocity at the rear boundaries is attributable to localized temperature elevations. As the air temperature rises, its density decreases, inducing a buoyancy-driven updraft along the walls that accelerates flow in the rear regions. Conversely, the reduced velocity in the central domain suggests the presence of a stagnation zone or pressure gradient distinct from the peripheral flow. Consequently, this flow profile implies an accelerated roasting at the rear and retarded roasting in the middle, assuming a uniform heat flux from the charcoal bed. Johansson (2015) explains the upward velocity proffer along the wall of a spray roaster reactor is due to hot air from burners rising in that region which is a result from the temperature distribution. The total average velocity in the roasting mesh's chamber was 0.962±0.17 m/s. The minimum velocity for the simulation is 0 m/s and the maximum is 1.806 m/s.

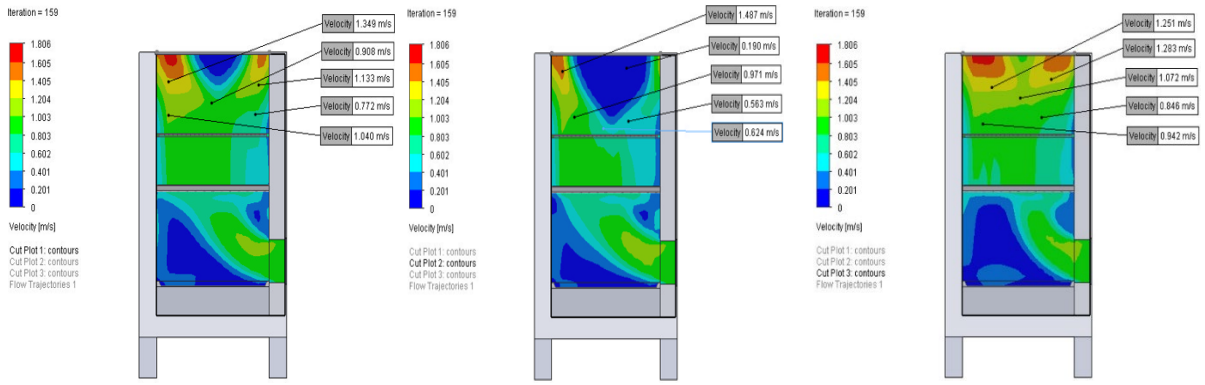

(a) (b) (c)

Figure 6: Air flow velocity cut plots at 1.5 m (a), 1.6 m (b) and 1.7 m (c) offsets

Table 3: Average velocity in the roasting chamber at different points

S/N	Velocity (m/s) at 1.5 m	Velocity (m/s) at 1.6 m	Velocity (m/s) at 1.7 m
1	1.349	1.487	1.251
2	0.908	0.190	1.284
3	1.133	0.971	1.072
4	0.772	0.563	0.846
5	1.040	0.624	0.942
	Average Velocity: 1.040±0.22	**Average Velocity: 0.767±0.49**	**Average Velocity: 1.079±0.19**
	Overall Average Velocity:	**0.962±0.17**	

3.4 Thermal efficiency

The average efficiency of the simulated heat of the roasting chamber is noticeably higher than that of the fabricated prototype as shown in Table 4. An average thermal efficiency of 93% was obtained for the simulated machine. However, the thermal efficiency of the fabricated prototype of the machine was 66%. The seemingly wide gap between the two thermal efficiencies might be due to the assumption of the use of a closed container for the simulated machine (which will reduce heat loss), whereas, the fabricated prototype (real life version)

Received: 17-01-2026 / Accepted: 02-02-2026 / Published: 31-03-2026

https://doi.org/10.70118/ujet.2026.0301.23

of the machine is with open top. The open top allowed some appreciable quantity of heat to escape during operation. This also explained that the simulated machine was assumed to be closed system with steady heat supply, while the fabricated machine operated as an open system. This situation is however not abnormal in roasting operation. Also, the absence of the maize cob in the simulation geometry led to an over-prediction of convective airflow and heat transfer efficiency. In addition, the part of the heat supplied to the maize cub must have been consumed due to water vapourisation (latent heat). The assumption of steady-state air supply in the model contrasted with the intermittent "fanning" airflow during the experiment, leading to a reduction in the effective heat transfer. The experimental heat source was non-constant due to charcoal degradation, whereas the model assumed a fixed temperature boundary. Also, the experimental results utilized an average temperature derived from all points, while the simulation analysis prioritized temperatures in the hotter regions, thereby skewing the comparison. Consideration of variable heat supply, latent heat of vapourisation in maize cob, and heat loss to the surrounding in the model would possibly correlate the model efficiency to the experimental run.

Table 4: Estimated simulation efficiency and fabricated machine efficiency

S/N	Simulation Efficiency	Fabricated Machine Efficiency
1	93 %	66 %

4.0 Practical Implications

Vivid conclusions of the research are presented in this section.

The CFD outcomes provided important guidelines for deign modification of the fabricated roasting machine. From the simulation, a high temperature profile was observed close to the top of the machine. This implies that the roasting mesh could be situated slightly close to the top where more uniform heating would be established. Also, the position of the blower could be repositioned in such a way that there would be elimination of stagnation point (regions where air velocity is low).

5.0 Conclusion

The roasting region of the simulated modelled machine performed best at the point 1.7 m cut plot. The overall average temperature and overall average air velocity of the simulated machine are 463.13 °C and 0.962 m/s, respectively. The simulated model of the machine is 93% efficient and fabricated prototype of the machine is 66% efficient. Hence, future modifications to enhance better thermal efficiency of the roasting operation is required.

6.0 Limitations

The limitations identified in this study includes the exclusion of maize cobs, assumption of steady-state heat transfer, closed-system operation in the model. Additionally, a mesh independence (grid sensitivity) study was not conducted due to computational limitations. Despite these limitations, the computational fluid dynamics identified the airflow trajectory and heat distribution in the roasting chamber, thereby providing valuable engineering perception about machine performance and redesign.

References

Adeyinka, I. T., Olayinka, R. A., Oyime, A. A., & Oluwaseun, K. (2014). *Development and performance evaluation of a maize roaster*. *2*(5), 161–164. https://doi.org/10.11648/j.ijsts.20140205.19

Atere, A. O., Adejuwon, S. O., Olalusi, A. P., & Olukunle, O. J. (2020). Modelling the Performance of a Roasting Machine. *American Journal of Engineering Research*, *9*(8), 75–82.

Bandyopadhyay, S., & Bhattacharya, R. (2014). *Discrete and Continuous Simulation: Theory and Practice*. CRC Press.

Bora, M. K., & Nakkeeran, S. (2014). Performance Analysis From The Efficiency Estimation of Coal Fired Boiler. *International Journal of Advanced Research*, *2*(5), 561–574.

Chiang, C., Wu, D., & Kang, D. (2017). Detailed Simulation Of Fluid Dynamics and Heat Transfer in Coffee Bean Roaster. *Journal of Food Process Engineering*, *1*(40), e12398. https://doi.org/10.1111/jfpe.12398

Dash, S., Mohanty, S., & Mishra, B. K. (2019). CFD modelling and simulation of an industrial scale continuous fluidized bed roaster. *Advanced Powder Technology*, *31*(2), 658–669. https://doi.org/10.1016/j.apt.2019.11.021

Dooley, K. (2002). Simulation Research Methods. In *Companion to organizations*. https://doi.org/10.1002/9781405164061.ch36

Fachruddin, F., Syafriandi, S., & Fadhil, R. (2021). Temperature coverage simulation of horizontal cylinder

type coffee roasting machine Temperature coverage simulation of horizontal cylinder type coffee roasting machine. *IOP Conference Series: Earth and Environmental Science*, *922*(1), 012031. https://doi.org/10.1088/1755-1315/922/1/012031

Jimoh, M. O., Ogunmoyela, O. A. B., & Ogabi, O. N. (2020). Development and Performance Evaluation of a Multi-Heat Source Plantain Roaster. *Nigerian Journal of Technological Development*, *17*(2), 120–126. https://doi.org/http://dx.doi.org/10.4314/njtd.v17i2.7

Johansson, S. (2015). *Towards Better Understanding of the Flow Inside Industrial Processes: a CFD Study*. Lule˚a University of Technology.

Kigozi, J., Akatukunda, D., Baidhe, E., Oluk, I., & Okori, F. (2020). Simulation of Heat Transfer in a Charcoal Soybean Roaster Using Computational Fluid Dynamics. *Journal of Basic and Applied Research International*, *26*(4), 33–38. https://doi.org/10.9734/bpi/rpst/v2/16893D

Lamé, G., & Simmons, R. K. (2018). From behavioural simulation to computer models : how simulation can be used to improve healthcare management and policy. *BMJ Simulation & Technology Enhanced Learning*, *6*(2), 1–8. https://doi.org/10.1136/bmjstel-2018-000377

Lisa, K., Abba, D. M., & Nura, A. (2019). Postharvest loss assessment of maize (Zea mays) along its value chain in Nigeria. *Journal of Stored Products and Postharvest Research*, *10*(1), 13–19.

Odewole, M. M., Sunmonu, M. O., Oyeniyi, S. K., & Adesoye, O. A. (2017). Computational fluid dynamics (CFD) simulation of hot air flow pattern in cabinet drying of osmo-pretreated green ball pepper. *Nigerian Journal of Technological Research*, *12*(1), 36–45. https://doi.org/10.4314/njtr.v12i1.7

Ogunlade, C. B., & Sangosina, M. I. (2019). Design, Fabrication and Evaluation of a Corn Roaster. *Proceedings of the 4th National Conference*, 1–7. http://eprints.federalpolyilaro.edu.ng

Özgün, O., & Barlas, Y. (2009). Discrete vs . Continuous Simulation : When Does It Matter ? *In Proceedings of the 27th International Conference of The System Dynamics Society*, *6*, 1–22.

Saeed, M. S., & Saeed, A. (2020). Health benefits of maize crop-An overview. *Current Research in Agriculture and Farming*, *1*(3), 5-8.

Silva, P. S., Trigo, A., Varajão, J., & Pinto, T. (2010). Simulation – Concepts and Applications. *Proceedings of the World Summit on Knowledge Society*, *September*, 429–434. https://doi.org/10.1007/978-3-642-16324-1_51

Sruthi, N. U., Premjit, Y., Pandiselvam, R., Kothakota, A., & Ramesh, V. (2021). An overview of conventional and emerging techniques of roasting: Effect on food bioactive signatures. *Food Chemistry*, *348*(January), 129088. https://doi.org/10.1016/j.foodchem.2021.129088

Suryadi, D., Leonanda, B. D., Mustagfirin, A., & Suandi, A. (2024). Analysis Of Temperature Distribution On The Coffee Roaster Drum For A Capacity Of 2 Kg Using Computational Fluid Dynamics (CFD) Dedi. *Jurnal Polimesin*, *22*(1), 2–6.

Szpicer, A., Bińkowska, W., Stelmasiak, A., Zalewska, M., Wojtasik-Kalinowska, I., Piwowarski, K., Piepiórka-Stepuk, J., & Półtorak, A. (2025). Computational fluid dynamics simulation of thermal processes in food technology and their applications in the food industry. *Applied Sciences*, *15*(1), 424. https://doi.org/10.3390/app15010424

Szpicer, A., Bińkowska, W., Wojtasik-Kalinowska, I., Salih, S. M., & Półtorak, A. (2023). Application of computational fluid dynamics simulations in food industry. *European Food Research and Technology*, *249*(6), 1411–1430. https://doi.org/10.1007/s00217-023-04231-y

White, K. P., & Ingalls, R. G. (2009). Introduction to Simulation . *Proceedings of the 2009 Winter Simulation Conference*, *April*, 1741–1755. https://doi.org/10.1109/WSC.2009.5429315

Received: 17-01-2026 / Accepted: 02-02-2026 / Published: 31-03-2026

https://doi.org/10.70118/ujet.2026.0301.23